Identification of the Internal Axial Ligand of HO_2−Cobalt(III)−Bleomycin: $^1H\{^{15}N\}$ HSQC NMR Investigation of Bleomycin, Deglycobleomycin, and Their Hydroperoxide−Cobalt(III) Complexes†

Chaunwu Xia, F. Holger Försterling, and David H. Petering*

Department of Chemistry, University of Wisconsin−Milwaukee, P.O. Box 413, Milwaukee, Wisconsin 53201

Received January 13, 2003

ABSTRACT: The identity of the axial ligand contributed by the drug in hydroperoxide−Co(III)−bleomycin and hydroperoxide−Co(III)−deglycobleomycin has been in doubt. With each structure, a combination of $^1H\{^{15}N\}$ HSQC and HMBC and ^1H COSY and NOESY NMR spectroscopy was used to observe and completely assign the nonaromatic ^{15}N chemical shifts of natural abundance bleomycin in the two hydroperoxide−Co(III) structures. Together with the ^{15}N assignments from a published 1D ^{15}N spectrum, the results permitted the assignment of the primary amine nitrogen to an axial ligand position in both structures.

The natural product bleomycin (Blm)[1] is a clinically useful antineoplastic drug (*1*−*4*). It is also one of a handful of proven metallodrugs in the cancer field (*5*, *6*). Bleomycin is a large, structurally heterogeneous molecule that includes regions that bind to DNA and to metal ions (Figure 1). Together, these structural elements support the formation of HO_2−Fe(III)Blm, which associates with double-stranded DNA and causes single and double strand cleavage and base release (*7*−*12*). Because of the difficulty in obtaining three-dimensional structural information about FeBlms, an intense effort has focused on understanding the structural properties of corresponding CoBlms, which have been hypothesized to be robust structural analogues of the FeBlm series (*13*−*27*). Structures of HO_2−Co(III)Blm bound to DNA oligomers containing a specific binding site of 5′-guanine-pyrimidine-3′ reveal that the metal domain and linker are folded into a unit that interacts with the minor groove edge of the guanine, while the drug's bithiazole is intercalated between adjacent base pairs. In the process, the hydroperoxide ligand becomes oriented toward the C4′-hydrogen of the deoxyribose that would be targeted if HO_2−Fe(III)Blm reacted with the oligomer (*19*, *22*, *25*−*27*).

Previous NMR studies support the hypothesis that HO_2−Co(III)Blm is a valid structural model for HO_2−Fe(III)Blm (*17*, *18*). Nevertheless, uncertainty still exists about features of the HO_2−Co(III)Blm structure. In particular, NMR studies have not defined the internal axial ligand to Co(III) that is provided by the drug. Neither has it been possible to locate the disaccharide unit with respect to the rest of the structure except that it is positioned on the same side of the cobalt coordination plane as the primary amine (*17*, *18*, *27*). It has been assumed that the primary amine serves as the axial ligand opposite the hydroperoxide, because it is ideally located to bind to Co(III), forming a five-membered, metal−ligand, ring system upon binding to the metal center (*8*, *17*, *18*). In perusing the rest of the Blm structure, after the in-plane ligands of Co(III) have been excluded (the nitrogens from the secondary amine, pyrimdine, amide, and imidazole), only the primary amine and mannose carbamoyl nitrogens are sterically accessible to the axial coordination position. Of these, the amine offers the stronger ligand for binding to the metal ion. Still, substitution of the carbamoyl nitrogen for the primary amine in the NMR structure calculation results in a structure that is as acceptable as the one with the primary amine ligand to Co(III) (*26*).

This assignment became ambiguous after the publication of the structure of HO_2−Co(III)−pepleomycin, based on a form of the drug that differs from Blm only in the nature of its variable R group (Figure 1). The published structure of HO_2−Co(III)−pepleomycin places the disaccharide carbamoyl group in the axial position (*28*). Strengthening this assignment, the authors found that when the mannose carbamoyl group could not act as the axial ligand in HO_2−Co(III)−deglycopepleomycin, the primary amine moved into this position (*28*). Having obtained more NMR information for this structure than that which supported the HO_2−Co(III)Blm A_2 structure, these results strongly challenged the assumption that the primary amine acts as the axial ligand. On the basis of this assignment, the relationship between the disaccharide and the metal coordination plane, which is unspecified in structures that place the primary amine in the internal axial ligand position, was also determined.

To reexamine the question of the nature of the axial ligand provided by the Blm drug, NMR experiments have been undertaken to assign and compare the ^{15}N spectra of Blm, dgBlm, HO_2−Co(III)Blm, and HO_2−Co(III)dgBlm. It was anticipated that large changes in the chemical shift of either the primary amine or carbamoyl nitrogens upon formation

† Supported by grants from the NIH (CA-22184) and the NSF (BIR-9512622).

* To whom correspondence should be addressed. E-mail: petering@uwm.edu.

[1] Abbreviations: Blm, bleomycin; dgBlm, deglycobleomycin; DQF-COSY, double-quantum-filtered correlation spectroscopy; HMBC, heteronuclear multiple bond correlation spectroscopy; HSQC, heteronuclear single-quantum correlation spectroscopy; NOESY, nuclear Overhauser effect spectroscopy.

10.1021/bi030016c CCC: $25.00
Published on Web 05/09/2003

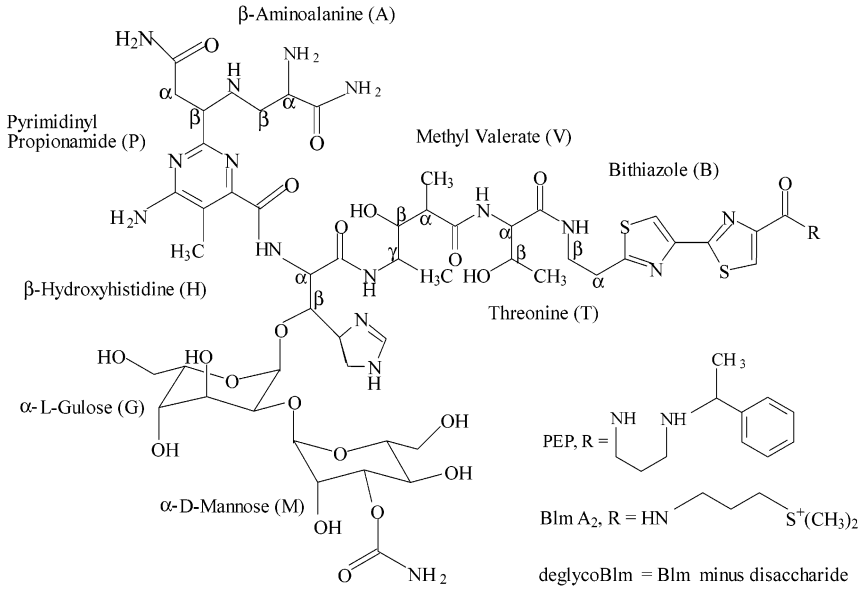

FIGURE 1: Structures of bleomycin, deglycobleomycin, and pepleomycin.

of the cobalt complexes would be observed and would signal its binding to the metal center.

MATERIALS AND METHODS

Sample Preparation. Metal-free bleomycin A_2 was purchased from Calbiochem and had a nominal purity of more than 85%. It was further purified by HPLC. This product was used as the starting material for the production of deglycobleomycin (dgBlm), which was made with minor modifications according to a published method (*29*). To convert these species to their Co(III) complexes, a 1.1-fold excess of $CoCl_2$ was added to rapidly stirred Blm A_2 or dgBlm A_2. With the Blm A_2 sample, stirring was completed after 30 min; with dgBlm A_2, it was continued for 24 h. During the dioxygenation and redox processes that occurred during the incubations, HO_2−Co(III)Blm A_2 and Co(III)-Blm A_2 or their deglyco counterparts form. They were efficiently separated by HPLC (*18*, *26*). Lyophilized Blm A_2, dgBlm A_2, HO_2−Co(III)Blm A_2, and HO_2−Co(III)dgBlm A_2 were dissolved in 0.55 mL of water containing 10% D_2O and 20 mM potassium phosphate buffer at pH 6.7 to attain a concentration of 10 mM. Samples were transferred to NMR tubes for the NMR experiments.

NMR Experiments. NMR spectra were acquired at 5 °C using a Bruker DRX500 NMR spectrometer operating at a proton frequency of 500.13 MHz and equipped with a triple axis gradient inverse broad-band (BBI) probe. Proton and nitrogen chemical shifts are reported relative to DSS and NH_3(liquid), respectively. Two-dimensional NOESY and DQF-COSY experiments were performed using standard methods. Natural abundance $^1H\{^{15}N\}$ HSQC experiments were performed with gradient selection and sensitivity enhancement employing water flip-back pulses to minimize saturation of exchanging protons. A typical experiment comprised 144 t_1 increments with 1024 transients of 2048 points each, covering a spectral width of 15205 and 8012 Hz in f_1 and f_2, respectively. $^1H\{^{15}N\}$ HMBC experiments were carried out using a standard gradient selected sequence with additional presaturation of the water resonance for improved water suppression. A total of 132 and 4096 data points were acquired in t_1 and t_2, respectively, with 1600 scans accumulated for each t_1 data point with a spectral width of 18245 and 8012 Hz in f_1 and f_2.

RESULTS

Proton Resonance Assignments. Blm A_2 and its hydroperoxide−Co(III) complex are comprised of a number of diverse structural elements (Figure 1, letters). dgBlm A_2 and HO_2−Co(III)dgBlm A_2 lack the disaccharide residue. A 2D NMR study of HO_2−Co(III)dgBlm A_2 has been reported (*30*). Although no interresidue NOEs were obtained, all of the proton chemical shifts were assigned. On the basis of the similarity in the chemical shifts and coupling constants, the authors posited that the structure of HO_2−Co(III)dgBlm A_2 was essentially the same as that of HO_2−Co(III)Blm A_2. In the present experiments, the use of high concentrations of HO_2−Co(III)dgBlm A_2 led to the definition of interresidue NOEs and the determination of its 3D structure as in previous studies (*17*, *18*). Indeed, the structure closely resembles that of HO_2−Co(III)Blm A_2 and will be reported elsewhere. The NMR ^1H chemical shifts of these four samples are listed in Table 1. For this work the proton chemical shifts of the disaccharide unit were not included. All of the chemical shifts of nitrogens attached to exchangeable protons in the hydroperoxy−Co(III) complexes, and most of them in the free drugs have also been assigned as described below.

Assignment of ^{15}N Chemical Shifts of the Amide and Amine Groups and the Related Exchangeable Proton Chemical Shifts. Isotopic enrichment of Blm with ^{15}N has not yet been achieved, so our experiments were performed with natural abundance drug in water solution by using 2D $^1H\{^{15}N\}$ HSQC NMR spectroscopic experiments. This approach is several orders of magnitude more sensitive than 1D ^{15}N NMR and yielded definitive resonance assignments of nitrogens with bound protons.

Figure 2 shows the 2D $^1H\{^{15}N\}$ HSQC NMR spectrum of HO_2−Co(III)Blm A_2. There are five NH and five major NH_2 peaks in the spectrum. It can be divided into three regions. At low field there are four NH peaks as seen in Figure 1s (top) (see Supporting Information). They are

Table 1: Proton (500 MHz) Chemical Shifts of Blm, dgBlm, HO_2−Co(III)Blm, and HO_2−Co(III)dgBlm. (5 °C)[a]

	complexes			
peaks	Blm	dgBlm	HO_2− Co(III)Blm	HO_2− Co(III)dgBlm
A_α	4.24	4.26	3.34	3.18
A_β	3.34	3.30	3.16	3.09
$A_{\beta'}$	3.25	3.23	2.66	2.77
$ACONH_{2a}$	8.08	8.08	7.78	7.88
$ACONH_{2b}$	7.54	7.53	6.99	7.24
ANH_{2a}			4.18	4.00
ANH_{2b}			3.14	3.91
ANH			5.92	6.26
P_α	2.86	2.84	3.43	3.50
$P_{\alpha'}$	2.79	2.78	3.12	3.12
P_β	4.26	4.22	5.04	5.16
PCH_3	1.95	1.92	2.39	2.52
$PCONH_{2a}$	7.76	7.76	7.99	7.95
$PCONH_{2b}$	7.12	7.06	7.28	7.18
PNH_{2a}			7.90	7.74
PNH_{2b}			7.68	7.47
H_α	5.04	4.85	4.91	4.80
H_β	5.46	5.22	5.45	5.37
H2	8.73	8.73	8.65	8.67
H4	7.54	7.47	7.53	7.55
HNH	9.13	9.16		
V_α	2.55	2.59	0.86	0.85
V_β	3.69	3.71	3.25	3.30
V_γ	3.87	3.85	3.44	3.45
$V_\alpha CH_3$	1.11	1.14	0.56	0.57
$V_\gamma CH_3$	1.09	1.10	0.92	0.94
VNH	8.44	8.49	8.82	9.16
T_α	4.16	4.18	4.32	4.30
T_β	4.02	4.04	4.19	4.12
TCH_3	1.03	1.05	1.14	1.12
TNH	8.18	8.30	8.87	8.95
B_α	3.21	3.25	3.16	3.21
$B_{\alpha'}$			2.99	3.06
B_β	3.59	3.61	3.76	3.76
$B_{\beta'}$			3.37	3.41
B5	8.18	8.15	8.10	8.08
B5′	7.98	8.01	7.76	7.81
BNH	8.42	8.46	8.52	8.43
S_α	3.34	3.37	3.29	3.31
S_β	2.11	2.14	2.06	2.08
S_γ	3.56	3.57	3.56	3.55
$S_{\gamma'}$			3.43	3.49
$S(CH_3)_2$	2.85	2.89	2.87	2.89
SNH	8.94	8.97	8.56	8.69
M-$CONH_{2a}$	6.57		6.72	
M-$CONH_{2b}$	6.22		6.11	

[a] Blm A_2, dgBlm A_2, HO_2−Co(III)Blm A_2, and HO_2−Co(III)dgBlm A_2 were dissolved in H_2O containing 10% D_2O and 20 mM potassium phosphate buffer at pH 6.7 to achieve 10 mM concentration.

(133.6, 8.82), (117.6, 8.52), (115.9, 8.56), and (114.4, 8.87) ppm. These four peaks can be readily identified as four secondary amide peaks according to the COSY spectrum (Figure 1s, bottom). In particular, the resonance at 8.87 ppm has one cross-peak with TαH at 4.32, so (114.4, 8.87) belongs to T−NH. Similarly, 8.82 has only one cross-peak with VγH at 3.44; thus, (133.6, 8.82) is assigned to V−NH. The resonance at 8.52 ppm has two cross-peaks with BβH and Bβ'H at 3.37 and 3.75, respectively. Hence, (117.55, 8.52) is associated with B−NH. Finally, 8.56 also has two cross-peaks with SγH and Sγ'H at 3.43 and 3.56. As such, (115.9, 8.56) is identified with S−NH.

In the middle part of the $^1H\{^{15}N\}$ HSQC spectrum, there are four major NH_2 peaks, (112.5/7.99, 7.28), (108.5/7.78, 6.99), (96.2/7.90, 7.68), and (76.1/6.72, 6.11) (Figure 2s, top).

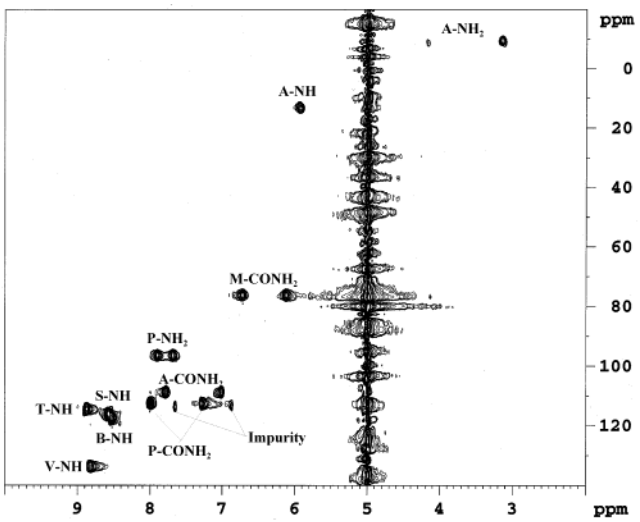

FIGURE 2: Contour plot of the $^1H\{^{15}N\}$ HSQC spectrum of HO_2−Co(III)Blm.

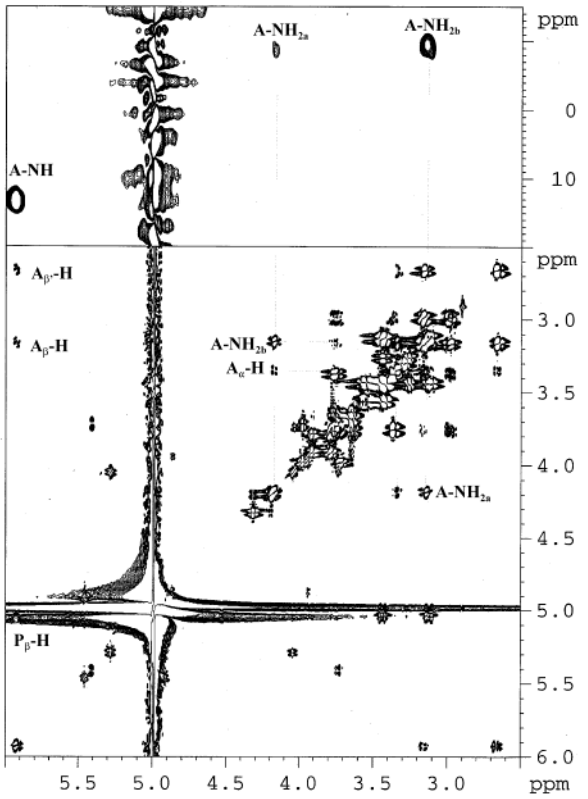

FIGURE 3: High-field region of the $^1H\{^{15}N\}$ HSQC spectrum of HO_2−Co(III)Blm (top) and its related DQF-COSY spectrum (bottom).

In the COSY spectrum (Figure 2s, bottom), 7.99 and 7.28, 7.78 and 6.99, 7.90 and 7.68, and 6.72 and 6.11 form four weak cross-peaks with each other. No other cross-peaks were found that related to these chemical shifts. Therefore, these four pairs of $^1H-^{15}N$ peaks should come from four isolated NH_2 groups, namely, A−$CONH_2$, P−$CONH_2$, M-CO−NH_2, and P−NH_2. The NOESY spectrum in Figure 3s shows that (7.99, 7.78) and (7.28, 6.99) also exhibit cross-peaks with AαH (3.34), AβH (2.67), Aβ'H (3.16), PαH (3.12), and Pα'H (3.43). Therefore, the two pairs of HSQC cross-peaks at (112.5, 7.99, 7.28) and (108.5, 7.78, 6.99) stem from A−$CONH_2$ and P−$CONH_2$. The cross-peaks between

Table 2: $^1H\{^{15}N\}$ HSQC Cross-Peaks of Bleomycin Species at 5 °C[a]

	Blm		dgBlm		HO_2−Co(III)Blm		HO_2−Co(III)dgBlm	
	^{15}N	^1H	^{15}N	^1H	^{15}N	^1H	^{15}N	^1H
S−NH	116.8	8.94	116.6	8.97	115.9	8.56	116.3	8.69
B−NH	119.4	8.42	119.4	8.46	117.6	8.52	117.9	8.43
T−NH	118.4	8.18	119.2	8.30	114.4	8.87	115.4	8.95
V−NH	133.9	8.44	136.0	8.49	133.6	8.82	133.7	9.16
H−NH	118.8	9.13	120.3	9.16	94.8[b]			
A−$CONH_2$	108.9	8.08/7.54	108.7	8.08/7.53	108.5	7.78/6.99	110.2	7.88/7.24
P−$CONH_2$	113.6	7.76/7.12	113.1	7.76/7.06	112.5	7.99/7.28	111.6	7.95/7.18
M−$CONH_2$	75.9	6.57/6.22			76.1	6.72/6.11		
P−NH_2	84.1[c]	6.49[b]			96.2	7.90/7.68	94.4	7.74/7.47
A−NH	35.1 or 36.5[d]				11.2	5.92	12.9	6.26
A−NH_2	36.5 or 35.1[c]				−9.7	4.18/3.14	−7.8	4.00/3.91

[a] Blm A_2, dgBlm A_2, HO_2−Co(III)Blm A_2, and HO_2−Co(III)dgBlm A_2 were dissolved in H_2O containing 10% D_2O and 20 mM potassium phosphate buffer at pH 6.7 to achieve 10 mM concentration. [b] H−H$^\beta$/N cross-peak in $^1H\{^{15}N\}$ HMBC. [c] The pH of the sample was adjusted to 6.4. [d] These chemical shifts are converted from ref *31*.

7.99 and 7.28 and PαH and Pα′H are much stronger than those between 7.78 and 6.99 and PαH and Pα′H, whereas those between 7.78 and 6.99 and AαH, AβH, and Aβ′H are more intense than the ones between 7.99 and 7.28 and these three hydrogens. Thus, the HSQC peaks at 7.78 and 6.99 were assigned to P−$CONH_2$ and the others to A−$CONH_2$. Besides these NOESY cross-peaks, A−$CONH_2$ and P−$CONH_2$ participate in many cross-peaks with the disaccharide protons in the 3.7−5.0 ppm region.

Resonances at 7.90 and 7.68 as well as 6.72 and 6.11 form four cross-peaks with P−CH_3 at 2.39; the former pair is very strong in the NOESY spectrum. Because P−NH_2 and P−CH_3 are neighboring substituents of the pyrimidine ring, the HSQC peak (96.2, 7.90, and 7.68) was assigned to P−NH_2 and the other (76.1, 6.72, and 6.11) to M−$CONH_2$. M−$CONH_2$ also establishes weak cross-peaks with P−NH_2 and very weak cross-peaks with AαH, AβH, and Aβ′H.

The high-field portion of the HSQC spectrum reveals one NH peak at (11.2/5.92) and one pair of NH_2 peaks at (−9.7/4.18, 3.14) as shown in Figure 3 (top). The NH peak can be identified as A−NH because the 5.92 ppm resonance forms cross-peaks with AβH (2.67) and Aβ′H (3.16) as well as with PβH (5.04) in the COSY spectrum. The NH_2 peaks belong to A−NH_2. In the COSY spectrum, the proton resonances assigned to ANH_2 (3.16, 4.18) generate cross-peaks with AαH (3.34) (Figure 3, bottom). The histidine NH is missing from the HSQC spectrum because the nitrogen is deprotonated upon ligation to the Co(III). However, there is a cross-peak between H−H$^\beta$ and a signal at 94.8 ppm in the $^1H\{^{15}N\}$ HMBC spectrum, which is due to the histidine amide nitrogen (data not shown).

The HSQC spectrum of HO_2−Co(III)dgBlm A_2 is very similar to that of its parent form, except that it does not have the M−$CONH_2$ cross-peaks (Figure 4). All of these peaks were assigned with the same strategy as used above and are listed in Table 2. The spectra in Figures 2 and 4 contain a pair of weak cross-peaks at (113.4, 6.85, 7.64) which result from an impurity of the solution, that was identified as CH_3-$CONH_2$. It is thought to be derived from the buffer solution used during the purification of the drug, which contained ammonium acetate.

The HSQC spectra of Blm A_2 and dgBlm A_2 resemble one another (Figures 4s and 5s). Combined with COSY and NOESY spectral data, the HSQC peaks have also been assigned and are listed in Table 2. There are several

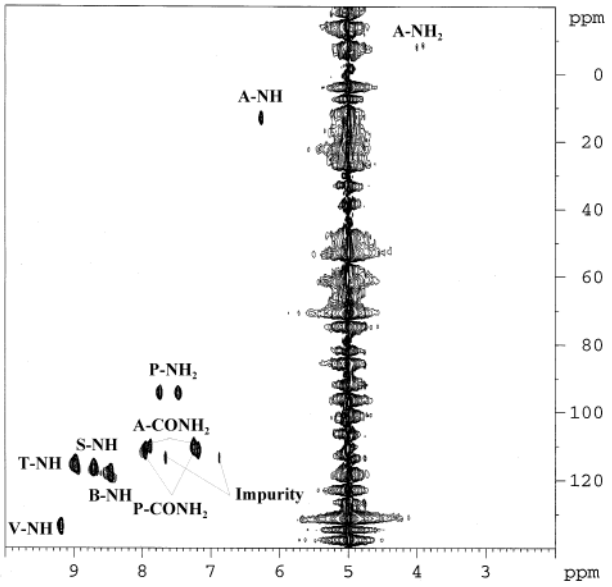

FIGURE 4: Contour plot of the $^1H\{^{15}N\}$ HSQC spectrum of HO_2−Co(III)dgBlm.

differences in comparison with the results for the cobalt complexes. First, five secondary amide cross-peaks were detected, including H−NH, which is deprotonated and does not appear in either the HO_2−Co(III)Blm A_2 or the HO_2−Co(III)dgBlm A_2 HSQC spectrum. Second, M−$CONH_2$ is weaker and does not have any cross-peaks with other protons in the NOESY spectrum. In addition, A−$CONH_2$ and P−$CONH_2$ display only intraresidue NOE cross-peaks. Also, the three amine peaks, A−NH_2, A−NH, and P−NH_2, are missing from the HSQC spectra of the free drugs, apparently, because of the fast exchange of their protons with the bulk water solvent under these conditions (pH 6.7). Slightly adjusting the pH to 6.4 reveals that the P−NH_2 protons of Blm A_2 are degenerate with a single cross-peak at (84.1, 6.49) in the HSQC spectrum (data not shown). The cross-peaks of A−NH_2 and A−NH remain missing. However, an early 1D ^{15}N NMR study of Blm A_2 in CH_3OH displayed all of the 17 nitrogen peaks (*31*). Except for the very high field peaks from nonprotonated nitrogens of bithiazole, pyrimidine, and imidazole rings, which cannot be detected by HSQC experiment, the ^{15}N chemical shifts in this report are very well correlated with those in 1D ^{15}N NMR experiments (Table 1s). Therefore, it can be reasonably

assumed that the ^{15}N chemical shifts of A−NH_2 and A−NH in metal-free Blm A_2, which were missing from our HSQC experiment, should be near 35.1 and 36.5 ppm, their positions in the 1D ^{15}N NMR spectrum.

DISCUSSION

The present experiments assign all of the ^{15}N NMR signals of nitrogens with bound hydrogens that are found in HO_2−Co(III)Blm A_2 and HO_2−Co(III)dgBlm A_2 as well as most of them in Blm A_2 and dgBlm A_2. Two key findings relate to the question of the identity of the internal axial ligand in HO_2−Co(III)Blm; both strongly support the identification of the primary amine as that ligand. First, the position of the mannose carbamoyl nitrogen (M−$CONH_2$) is only marginally perturbed upon complexation of Blm A_2 with HO_2−Co(III) (75.9 vs 76.1 ppm). If it were bound to Co(III), a large shift would be expected. Second, the positions of the primary and secondary amine nitrogens (A−NH_2 and A−NH) at −9.7 and 11.2 ppm, respectively, are highly shifted in comparison with metal-free primary and secondary amines (Table 2). The apparent large upfield shifts of A−NH_2, A−NH, and H−N (amide) in HO_2−Co(III)Blm A_2 are completely consistent with their direct complexation to a positively charged metal ion (*32*). The similarity in ^{15}N chemical shifts of HO_2−Co(III)Blm A_2 and HO_2−Co(III)-dgBlm A_2 also supports the identification of the primary amine as the internal axial ligand in HO_2−Co(III)Blm A_2, because in HO_2−Co(III)dgBlm A_2, the primary amine is the only possible axial ligand. In addition, the missing H−NH HSQC peak confirmed that an amide nitrogen is deprotonated when bound to Co(III). The relatively large ^{15}N chemical shifts of P−NH_2 in metal-free Blm A_2 (84.1 ppm) and the Co(III) complex (96.2 ppm) are in agreement with the direct ligation of the aromatic pyrimidine ring nitrogen with the metal center.

Review of the NMR study that led to the definition of the mannose carbamoyl nitrogen as the axial ligand in HO_2−Co(III)−pepleomycin shows that this result largely depended upon the accurate assignment of the A−NH_2 proton chemical shifts in HO_2−Co(III)−pepleomycin (6.58, 5.93 ppm) and HO_2−Co(III)−deglycopepleomycin (4.09, 3.97 ppm) (*33*). It was primarily these differences which led the authors to suggest the carbamoyl group as the axial ligand of HO_2−Co(III)−pepleomycin. Unfortunately, no detail was provided about the method of assignment. In contrast, the chemical shifts for the primary amine for HO_2−Co(III)Blm A_2 (4.18, 3.14) and HO_2−Co(III)dgBlm A_2 (4.00, 3.91), resulting from unambiguous assignments in the present study, are similar and do not warrant the conclusion that the primary amine is a metal-binding ligand only in the deglyco form. According to our interpretation, the differences in chemical shift are due to the presence or absence of the disaccharide in the vicinity of the primary amine hydrogens. In the pepleomycin work it was also asserted that the fast exchange rate of A−NH_2 protons (very broad NMR peaks) in HO_2−Co(III)−pepleomycin and the slower exchange rate in its deglyco analogue indicated the same difference in axial ligation for HO_2−Co(III)−pepleomycin and HO_2−Co(III)−deglycopepleomycin. However, because the spectra were acquired at different pH values (6.9 and 6.4, respectively), the difference in the exchange rate may simply be due to the change in pH.

Another case in which the carbamoyl group and not the primary amine was defined as the axial ligand is OC−Fe(II)Blm A_2 (*33*). This conclusion was based primarily on the large upfield shifts of the mannose C3−H resonance from 4.68 ppm in metal-free Blm to 4.21 ppm in its metal complex and the NOEs between the M and H residues, which required that the M group is close to the metal center. However, proton chemical shifts can depend on a variety of long-range environmental effects apart from metal complexation. Therefore, proton chemical shift difference alone cannot determine the ligation state. Moreover, the many NOE connections between disaccharide and metal domain hydrogens that were observed in the present study are also consistent with the location of the disaccharide in close proximity to the equatorial coordination plane of the Co(III) center.

The placement of the primary amine in the axial position above the Co(III) coordination plane instead of the mannose carbamoyl nitrogen removes the only conformational determinant [the carbamoyl nitrogen−Co(III) bond] that locates the disaccharide with respect to the metal domain of HO_2−Co(III)−pepleomycin and OC−Fe(II)Blm. However, the accurate assignment of the exchangeable ^1H resonances of HO_2−Co(III)Blm A_2 by $^1H\{^{15}N\}$ HSQC NMR spectroscopy has uncovered a number of NOE interactions that provide the basis for rigorously defining the orientation of the disaccharide unit with respect to the rest of the drug. Work on a refined structure of HO_2−Co(III)Blm A_2 that includes this relationship is currently in progress.

SUPPORTING INFORMATION AVAILABLE

One table giving ^{15}N NMR resonances of bleomycin A_2 and five figures showing the low- and middle-field regions of the $^1H\{^{15}N\}$ HSQC and DQF-COSY spectra of HO_2−Co(III)Blm and contour plots of the partial NOESY spectrum of HO_2-Co(III)Blm and of the $^1H\{^{15}N\}$ HSQC spectra of free Blm and dgBlm. This material is available free of charge via the Internet at http://pubs.acs.org.

REFERENCES

1. Umeazwa, H., Maeda, K., Tekeuchi, T., and Okami, J. (1966) *J. Antibiot. 19*, 200−209.
2. Umezawa, H., Suhara, Y., Takita, T., and Maeda, K. (1967) *J. Antibiot. 20*, 15−24.
3. Fujii, A., Takita, T., Shimada, N., and Umezawa, H. (1974) *J. Antibiot. 20*, 73−77.
4. Sikic, B. I., Rozencweig, M., and Carter, S. K., Eds. (1985) *Bleomycin Chemotherapy*, Academic Press, Orlando, FL.
5. Powis, G. (1991) *The Toxicity of Anticancer Drugs* (Powis, G., and Hacker, M. P., Eds.) Chapter 1, Pergamon Press, New York.
6. Lazo, J. S., and Chabner, B. A. (1996) *Cancer Chemotherapy and Biotherapy: Principles and Practice* (Chabner, B. A., and Longo, D. L., Eds.) 2nd ed., Lippincott-Raven, Philadelphia, PA.
7. Petering, D. H., Mao, Q., Li, W., DeRose, E., and Antholine, W. E. (1996) *Met. Ions Biol. Syst. 33*, 619−648.
8. Stubbe, J., Kozarich, J. W., Wu, W., and Vanderwall, D. E. (1996) *Acc. Chem. Res. 29*, 322−330.
9. Claussen, C. A., and Long, E. C. (1999) *Chem. Rev. 99*, 2797−2816.
10. Burger, R. M. (1998) *Chem. Rev. 98*, 1153−1169.
11. Byrnes, R. W., Templin, J., Sem, D., Lyman, S., and Petering, D. H. (1990) *Cancer Res. 50*, 5275−5286.
12. Radtke, K., Lornitzo, F. A., Byrnes, R. W., Antholine, W. E., and Petering, D. H. (1994) *Biochem. J. 302*, 655−664.
13. Sugiura, Y. (1980) *J. Am. Chem. Soc. 102*, 5208−5212.
14. Chikira, M., Antholine, W. E., and Petering, D. H. (1989) *J. Biol. Chem. 264*, 21478−21480.

15. Xu, R. X., Antholine, W. E., and Petering, D. H. (1992) *J. Biol. Chem. 267*, 944−949.
16. Xu, R. X., Antholine, W. E., and Petering, D. H. (1992) *J. Biol. Chem. 267*, 950−955.
17. Xu, R. X., Nettesheim, D., Otvos, J. D., and Petering, D. H. (1994) *Biochemistry 33*, 907−916.
18. Wu, W., Vanderwall, D. E., Lui, S. M., Tang, X.-J., Turner, C. J., Kozarich, J. K., and Stubbe, J. (1996) *J. Am. Chem. Soc. 118*, 1268−1280.
19. Wu, W., Vanderwall, D. E., Turner, C. J., Kozarich, J. W., and Stubbe, J. (1996) *J. Am. Chem. Soc. 118*, 1281−1294.
20. Mao, Q., Fulmer, P., Li, W., DeRose, E., and Petering, D. H. (1996) *J. Biol. Chem. 271*, 6185−6191.
21. Fulmer, P., Zhao, C., Li, W., DeRose, E., Antholine, W. E., and Petering, D. H. (1997) *Biochemistry 36*, 4367−4374.
22. Vanderwall, D. E., Lui, S. M., Wu, W., Turner, C. J., Kozarich, J. W., and Stubbe, J. (1997) *Chem. Biol. 4*, 373−386.
23. Li, W., Zhao, C., Xia, C., Antholine, W. E., and Petering, D. H. (2001) *Biochemistry 40*, 7559−7568.
24. Rajani, C., Kincaid, J. R., and Petering, D. H. (2001) *Biophys. Chem. 94*, 219−236.
25. Hoehn, S. T., Junker, H. D., Bunt, R. C., Turner, C. J., and Stubbe, J. (2001) *Biochemistry 40*, 5894−5905.
26. Zhao, C., Xia, C., Mao, C., Försterling, H., DeRose, E., Antholine, W. E., Subczynski, W. K., and Petering, D. H. (2002) *J. Inorg. Biochem. 91*, 259−268.
27. Wu, W., Vanderwall, D. E., Turner, C. J., Hoehn, S., Chen, J., Kozarich, J. W., and Stubbe, J. (2002) *Nucleic Acids Res. 30*, 4881−4891.
28. Caceres-Cortes, J., Sugiyama, H., Ikudome, K., Saito, I., and Wang, A. H.-J. (1997) *Eur. J. Biochem. 244*, 818−828.
29. Kenani, A., Lamblin, G., and Henichart, J. P. (1988) *Carbohydr. Res. 177*, 81−89.
30. Wu, W., Vanderwall, D. E., Teramoto, S., Hoehn, S. T., Lui, S. M., Tang, X.-J., Turner, C. J., Boger, D. L., Kozarich, J. K., and Stubbe, J. (1998) *J. Am. Chem. Soc. 118*, 2239−2250.
31. Naganawa, H., Takita, T., Umezawa, H., and Hull, W. E. (1979) *J. Antibiot. 32*, 539−541.
32. Juranić, N., Vuk-Pavlović, S., Nikolić, A. T., Chen, T.-B., and Macura, S. (1996) *J. Inorg. Biochem. 62*, 117−126.
33. Akkerman, M. A. J., Neijman, E. W. J. F., Wijmenga, S. S., Hilbers, C. W., and Bermel, W. (1990) *J. Am. Chem. Soc. 112*, 7462−7474.

BI030016C